Large Eddy Simulation of a Turbulent Jet

A. T. Webb[1] and N. N. Mansour[2]

[1]School of Civil Engineering
Australian Defense Force Academy, UNSW, ACT, 2600 AUSTRALIA
[2]Center for Turbulence Research ,
NASA Ames Research Center, CA 94035, USA

Abstract

Here we present the results of a Large Eddy Simulation of a non-buoyant jet issuing from a circular orifice in a wall, and developing in neutral surroundings. The effects of the subgrid scales on the large eddies have been modeled with the dynamic large eddy simulation model applied to the fully 3D domain in spherical coordinates. The simulation captures the unsteady motions of the large-scales within the jet as well as the laminar motions in the entrainment region surrounding the jet. The computed time-averaged statistics (mean velocity, concentration, and turbulence parameters) compare well with laboratory data without invoking an empirical entrainment coefficient as employed by line integral models. The use of the large eddy simulation technique allows examination of unsteady and inhomogeneous features such as the evolution of eddies and the details of the entrainment process.

Introduction

Standard engineering design models for jets and plumes employ averaging techniques that mask the rich details evident in the real world. A snapshot of a plume billowing from a chimney or effluent discharging from an ocean outfall shows a highly irregular edge with regions of low concentration near the centre and pockets of high concentrations far downstream from the source. Superimposed on this irregularity is a structure evidenced by the boils or eddies which seem to repeat at seemingly regular intervals. While experimental techniques are available to explore these unsteady phenomena, sampling is limited. For example laser-doppler anemometry is a point method that misses the synoptic, while laser-induced fluorescence and particle-imaging velocimetry only provide a slice of information with sampling limited to the frame rate of the video camera and the density of pixels in the charged couple device. An attractive alternative is to model the fluid motions at a sufficiently detailed scale so that the energy-containing eddies are resolved – this modeling approach is called Large Eddy Simulation (LES). We present here the results of such a study on a simple momentum jet discharging into a semi-infinite quiescent environment.

The Model

The equations to be solved are the filtered incompressible Navier-Stokes equations together with the continuity equation and a scalar transport equation representing a passive tracer (or pollutant).

The non-dimensional governing parameters for this flow are:

$$\text{Reynolds number} \quad = \quad Re \quad = \quad U_0 D_0/\nu \; ,$$
$$\text{Prandtl number} \quad = \quad Pr \quad = \quad \nu/\kappa \; ,$$

where U_0 is the mean vertical velocity of the fluid leaving the source (used to non-dimensionalise all velocities), D_0 is the diameter of the orifice (used to non-dimensionalise lengths), ν is the kinematic viscosity of the fluid, and κ the scalar diffusivity. In the following we use T to represent the dimensionless scalar concentration (e.g. a tracer or pollutant).

Large Eddy Simulation

To create an LES computational model, the Navier-Stokes/continuity/tracer equations are filtered with the filter cutoff chosen to remove the dissipative scales but retain the energy-containing scales. In the present study, the subgrid scales stresses and fluxes are modeled using the dynamic approach ([6], and [4]), which automatically determines, using different filter widths, the spatial distribution of the magnitude of eddy viscosity as required by the subgrid-scale Smagorinsky model. This procedure obviates the need for any empirical determination of the Smagorinsky constant.

A major advantage of this method is that it is much more likely to be successful for inhomogeneous flows, particularly in the present case where part of the domain is laminar. This issue was explored by Liu et al. [9] who compared the Smagorinsky and the dynamic models with particle image velocimetry laboratory measurements in the far field of a turbulent round jet. The Smagorinsky model was found to correlate poorly with the real turbulent stress, while the dynamic model yielded appropriate coefficients. The inadequacy of the Smagorinsky model was also demonstrated by Bastiaans et al. [1] in an LES model of transient buoyant plumes in an enclosure. In this study, they found they could only get a match of the evolving plume by tuning the Smagorinsky constant. Such tuning reduces the generality of a model.

Numerical scheme

We use the LES code of Boersma, an adaptation of his own jet direct numerical simulation (DNS) code[3]. The code was modified by Basu [2] to compute buoyant plumes. A spherical polar coordinate system (R, θ, ϕ; along the radial, lateral and azimuthal directions respectively) is used here because, for the present flow with its conical mean growth, a spherical coordinate system allows for a well-balanced resolution of the flow field without excessive grid points. For presentation purposes, however, and for comparison to laboratory data, the results are converted to the axisymmetric cylindrical coordinate system (z axial and r radial). The symbols U and V are used for velocities in the z and r directions respectively. Further details of the computational scheme can be found in [3], [4], and [6].

Boundary conditions and test parameters

For the chosen staggered grid, only velocities normal to the boundary need be specified - i.e. six components. The equation for the tracer (T) is second order in each spatial direction, requiring six boundary conditions as well.

For the bottom boundary a Dirichlet BC is used with log-law profile velocity at the orifice, to which white noise of 2% rms is added. At the outflow boundary, or the top end of the current computational domain, we use the advective boundary condition and at the lateral boundary we apply a stress-free condition ([3] and [7]). Periodic boundary conditions are used along the azimuthal ϕ direction boundaries and lateral velocity (u_θ) is set to mean value at $\theta = 0$.

The Reynolds number for the jet source is set at 3500 – within the range of experimental data for which the jet is turbulent at or near the nozzle[5].

The computations are carried out in a domain that extends to 50 diameters downstream of the source. The domain encompasses a conical volume of lateral angle $\pi/12$, with a virtual origin that is 15 diameters upstream of the orifice. For the purpose of LES, this volume is discretised using a grid of size ($N_r = 128, N_\theta = 40, N_\phi = 32$). Time stepping is chosen to satisfy CFL conditions [3] which turns out to be typically 0.01 in dimensionless time units (D_0/U_0). Spatially the grid is an order of magnitude smaller than the expected large scale (typically $0.4z$, although there is an arbitrariness about the definition of the jet edge) and an order of magnitude larger than the Kolmogorov length scale [10] as appropriate for LES modeling. The temporal sampling is much smaller than the Kolmogorov time scale.

The computations are carried out for over 100,000 time-steps (a non-dimensional time of about $t = 300$). Averaging for statistical quantities was done towards the end of the simulations when we were convinced that the flow was statistically stationary.

Model verification

Confidence in the model can only come from comparison with laboratory data. There is a wealth of such data and we use a selection reviewed by List[8]. The data represent air in air and water in water over a wide range of Reynolds number (but all in the turbulent regime). Despite the range of fluids and laboratory conditions there is a surprising consistency between the results and hence we would expect our model to be able to match them well.

To compare the model results, we have averaged first moment and second moment statistics over some 10,000 samples. The particular sampling and averaging carried out yields an uncertainty of about 2% for any given statistical estimate.

Here we examine two statistics, the mean z-direction velocity (U) and the tracer concentration (T). The procedure for reducing the data was to fit Gaussian curves (using Matlab's routine nlinfit with emphasis on the inner radius) to the r-direction profiles. The fitted e-folding radius (r_e) and the fitted maximum value were used to scale the data. Of the many checks that we have made [11], we here present just two – we recall that the experimental jet e-folding width grows linearly as $0.107z$ for U and $0.126z$ for T. (From the laboratory data the uncertainty for the growth rates is 3% for both U and T [8]).
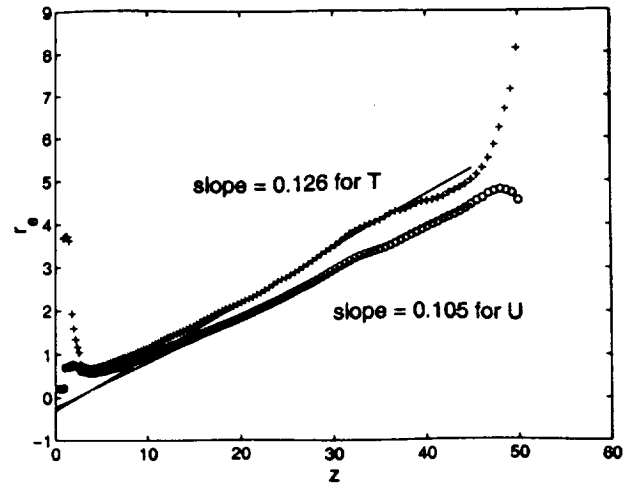

Figure 1: Growth of jet width in terms of the e-folding width for z-direction velocity (circles) and tracer (crosses).

The fitted slopes in the central region (beyond the ZFE and short of the apparent influence of the downstream boundary) are 0.105 for U and 0.126 for T (figure 1). The matches are remarkably close to the laboratory data and well within the data uncertainty.

Other checks carried out [11] show that the centerline velocity and tracer decay as z^{-1}, and that turbulent fluctuations and turbulent momentum and scalar transport match laboratory data. In almost every case the match is well within data and model uncertainty. We also verified that most of the variance can be accounted for by the resolved portion of the model – as we would hope from an LES model.

Unsteady features

To examine some of the jet features we take sections both through the centerline (meridional) and across the jet (radial). At the computer, it is instructive to roam through many such sections but even with just two we can see a great deal. Figure 2a is a meridional section between 6 and 13 diameters from the source while figure 2b is a radial section at about 9 diameters from the source. We overlay the instantaneous tracer concentrations and velocity vectors.

At the bottom centre of the meridional section (figure 2a), between $z = 6$ and $z = 8$, we can see what at first sight appears to be a core region of almost source concentration with velocities matching the source velocity. There is actually a peak concentration at $z = 6.7$, $r = -0.2$ that is at the center of a patch about to break from the core to form a more or less separate puff. Such puffs are shed repeatedly, and, in fact, the previously formed puff can be seen at $z = 11$. Given that the source is uniform and steady with the addition of a small level of noise it is remarkable how unsteady and irregular are the features.

Within and about these large scale puffs are eddies of comparable scale. An anti-clockwise eddy with horizontal axis can be seen centered at $z = 9$, $r = -1$. At its top this eddy transports jet fluid away from the core while at the bottom, ambient fluid is transported towards the jet center. The horizontal extent of the eddy and its three-
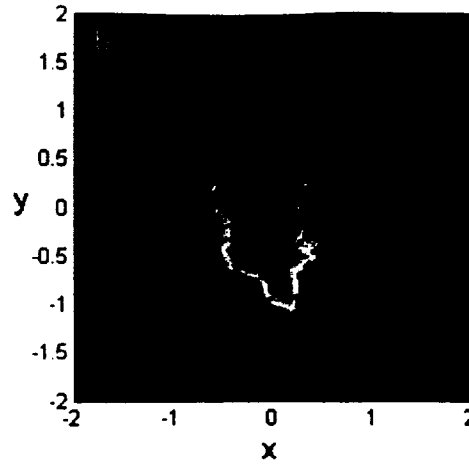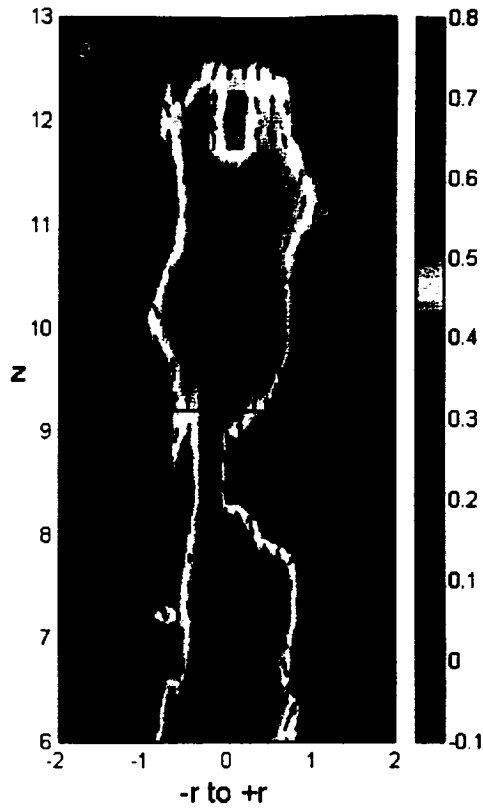
Figure 2: Instantaneous meridional (a) and radial (b) sections of tracer concentration and velocity vectors. The relative position of each section is indicated by a black line.

dimensional character is evident from the radial section (Figure 1b) at $x = -1.5$, $y = -0.8$. An example of an eddy with vertical axis can be seen in the radial section centered at $x = 1.2$, $y = 0$. As with the other eddy, this one is clearly advecting away core fluid in the outward portion and ambient fluid towards the center in the inward portion. Closer to the core, there appear to be several smaller scale eddies which further mix the jet fluid with ambient. Image sequences show that any jet fluid that strays too far from the center is readily re-entrained by the sink flow that exists outside the turbulent jet region.

Although we have been emphasizing the irregularity of the flow, there is an underlying apparent dominant size of the puffs and eddies, and a typical frequency at which the puffs are shed. In the following we look to quantifying these scales.

Quantifying scale

In an attempt to quantify the time scale we have examined a time series of tracer concentration at a single point – on the centerline at 30 diameters from the source. This choice is arbitrary as any point should share the same temporal spectral characteristics. A raw spectrum is computed from a sequence of duration 460 time units at interval of 1.8 time units. Band averaging over 4 adjacent estimates reduces the uncertainty (figure 3). Although this still leaves broad confidence intervals, a clear peak is evident at 0.025 dimensionless frequency units (U_0/D_0). There may also be other peaks at about 0.07 and 0.1 for which we offer three possible explanations – (1) they are just noise – note that we only use a 4-fold
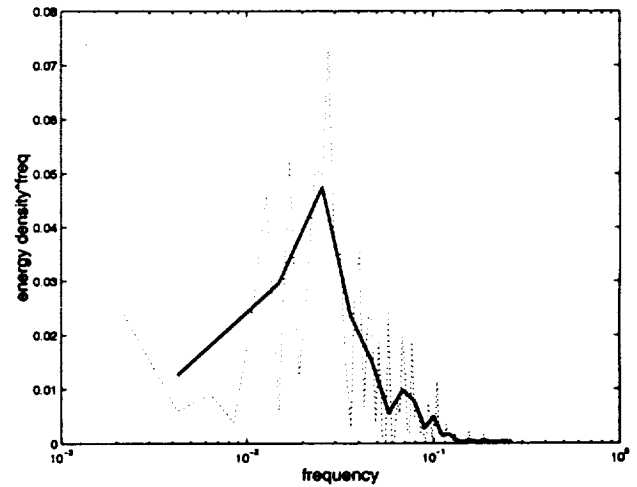

Figure 3: Spectrum of tracer at $z = 30$. The dashed line is the raw spectrum, while the solid is band-averaged.

band-average, (2) they represent real higher frequency motions – (3) they are spurious peaks associated with the non-sinusoidal shape of the puffs. We will have more to say about this with regard to the spatial spectrum.

From the mean flow field one could invoke the Taylor frozen-field assumption to deduce a spatial scale, but an impediment to computing such a scale is the obvious inhomogeneity. However, we can make use of the scaling determined from the mean and variance to transform an axial sample of the tracer to a homogeneous equivalent.
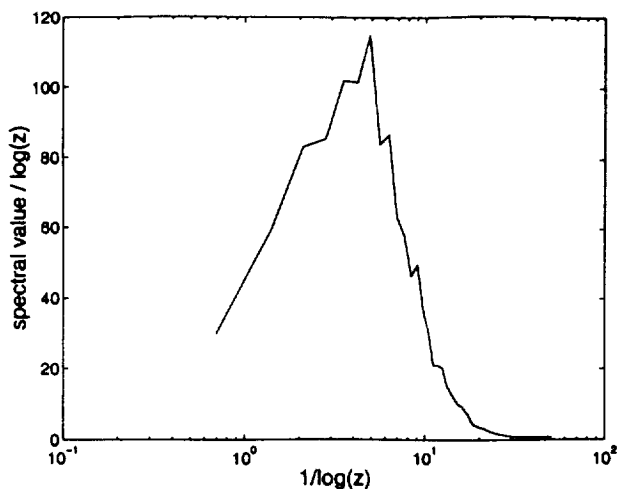
Figure 4: Spectrum of centerline scalar concentration in homogeneous transformed space

Subtracting the mean centerline temperature and then dividing by the mean removes these two trends but still leaves a z-dependent wavelength. However, if we transform the z-axis by the antiderivative of the expected inverse growth rate, the z-dependence is removed. In this case, the growth is expected to be linear, and hence the transformation is simply logarithmic. The spectra of 100 such records were averaged to yield the spectrum shown in figure 4.

The interpretation of the peak at 5 transformed wave number units is that the centerline eddy length is proportional to distance from the source and is here equal to $0.2z$. Curiously this measure of the large scale motion matches the mean jet width defined by the e-folding half – i.e. the energy containing eddies are the same order of magnitude as the jet itself.

The secondary peaks at 6.2 and 9 are reminiscent of those seen in the temporal spectrum (figure 3), except here, with the narrow uncertainty, we are sure they are not noise. Of the other two possible explanations (real higher wavenumber features or spurious peaks) we are convinced that the latter is the correct one. An examination of a centerline tracer record shows that the head of a puff is generally steeper than the tail. A spectrum computed from an artificially generated monochromatic wave with such an asymmetry recreates the spurious peaks seen here.

Conclusion

The LES of a simple jet does a remarkable job of simulating laboratory experiment data without the need to invoke empiricism such as an entrainment coefficient. Inclusion of the large eddies in the model allows one to examine the detail of the entrainment process. The behaviour of the jet is that of a series of puffs rather than a steady stream. The outward motion at the top of the puff together with the inward motion at the bottom acts to interchange jet fluid with ambient and smaller scale motions. The axes of the eddies are not constrained, however, to the lateral direction as eddies are also evident with axes at orthogonal orientation. A transformation of centerline tracer concentration yields an estimate of the large scales of the unsteady motions. For the case examined here, this turns out to scale with distance from

the source, and to be about the same size as the mean width of the jet. Whether this result is Reynolds number dependent remains to be seen.

References

[1] Bastiaans R.J.M., C.C.M. Rindt, A.A. van Steenhoven, and Nieuwstadt, Direct and large-eddy simulations of transient buoyant plumes: a comparison with an experiment, in P.R. Voke et al. (eds), *Direct and Large-Eddy Simulation I*, 399-410, Kluwer Academic Publishers, 1994.

[2] Basu A.J. and N.N. Mansour, Large Eddy Simulation of a forced round turbulent buoyant plume in neutral surroundings, *Center for Turbulence Research Annual Research Briefs*, NASA Ames Research Center/ Stanford Univ., 239-248, 1999.

[3] Boersma B.J., G. Brethouwer, and F.T.M. Nieuwstadt, A numerical investigation on the effect of the inflow conditions on the self-similar region of a round jet, *Phys. Fluids* 10, 899-909, 1998.

[4] Cabot W. and P. Moin, Large eddy simulation of scalar transport with the dynamic subgrid-scale model, in *Simulation and modelling of turbulent flows*, (ed. Gatski T.B., M.Y. Hussaini, J.L. Lumley), Oxford University Press,1996.

[5] Chen C.J. and W. Rodi, *Vertical turbulent buoyant jets, a review of experimental data*, HMT, the science and applications of heat and mass transfer, vol. 4, Pergamon Press, 1980.

[6] Germano M., U. Piomelli, P. Moin and W.H. Cabot, A dynamic subgrid-scale eddy viscosity model, *Phys. Fluids* A3, 1760-1765, 1991.

[7] Gresho P.M., Incompressible fluid dynamics : some fundamental formulation issues, *Ann. Rev. Fluid Mech.* 23, 413-454, 1991.

[8] List E.J., Mechanics of turbulent buoyant jets and plumes, in W. Rodi (ed) Turbulent buoyant jets and plumes, HMT, the science and applications of heat and mass transfer, vol. 6, Pergamon Press, 1-68, 1982.

[9] Liu S., C. Meneveau and J. Katz, Experimental study of similarity subgrid-scale models of turbulence in the far-field of a jet, in P.R. Voke et al. (eds), *Direct and Large-Eddy Simulation I*, 37-48, Kluwer Academic Publishers, 1994.

[10] Papantoniou D. and E.J. List, Large scale structure in the far field buoyant jets, *J. Fluid Mech.* **209**, 151-190, 1989.

[11] Webb A.T. and N.N. Mansour, Towards LES models of jets and plumes, *Center for Turbulence Research Annual Research Briefs*, NASA Ames Research Center/Stanford Uni., 229-240, 2000.